Understanding deterministic diffusion by correlated random walks

2002 J. Phys. A: Math. Gen. 35 4823

(http://iopscience.iop.org/0305-4470/35/23/302)

INSTITUTE OF PHYSICS PUBLISHING JOURNAL OF PHYSICS A: MATHEMATICAL AND GENERAL

J. Phys. A: Math. Gen. **35** (2002) 4823–4836 PII: S0305-4470(02)34259-8

Understanding deterministic diffusion by correlated random walks

R Klages and N Korabel

Max Planck Institute for Physics of Complex Systems, Nöthnitzer Strasse 38, D-01187 Dresden, Germany

E-mail: rklages@mpipks-dresden.mpg.de and korabel@mpipks-dresden.mpg.de

Received 21 February 2002
Published 31 May 2002
Online at stacks.iop.org/JPhysA/35/4823

Abstract

Low-dimensional periodic arrays of scatterers with a moving point particle are ideal models for studying deterministic diffusion. For such systems the diffusion coefficient is typically an irregular function under variation of a control parameter. Here we propose a systematic scheme of how to approximate deterministic diffusion coefficients of this kind in terms of correlated random walks. We apply this approach to two simple examples which are a one-dimensional map on the line and the periodic Lorentz gas. Starting from suitable Green–Kubo formulae we evaluate hierarchies of approximations for their parameter-dependent diffusion coefficients. These approximations converge exactly yielding a straightforward interpretation of the structure of these irregular diffusion coefficients in terms of dynamical correlations.

PACS numbers: 05.45.Ac, 05.60.Cd, 05.10.−a, 05.45.Pq, 02.50.Ga

(Some figures in this article are in colour only in the electronic version)

1. Introduction

Deterministic diffusion is a prominent topic in the theory of chaotic dynamical systems and in non-equilibrium statistical mechanics [1, 2]. To achieve a proper understanding of the mechanism of deterministic diffusion with respect to microscopic chaos in the equations of motion, a number of simple model systems was proposed and analysed. An interesting finding was that, for a simple one-dimensional chaotic map on the line generalizing random walk diffusion in terms of including dynamical correlations, the diffusion coefficient is a fractal function of a control parameter [3–5]. Diffusion coefficients exhibiting similar irregularities are also known for more complicated systems such as sawtooth maps [6], standard maps [7] and Harper maps [8], the latter two models being closely related to physical systems such as the kicked rotor, or a particle moving in a periodic potential under the influence of

electric and magnetic fields. More recently, related irregularities in the diffusion coefficient were discovered in Hamiltonian billiards such as the periodic Lorentz gas [9], and for a particle moving on a corrugated floor under the influence of an external field [10]. That this phenomenon is not specific to diffusion coefficients is suggested by results on other transport coefficients such as chemical reaction rates in multibaker maps [11], electrical conductivities in the driven periodic Lorentz gas [12], and magnetoresistances in antidot lattices [13] which, again, exhibit strongly irregular behaviour under parameter variation.

In this paper we wish to contribute to the further analysis and understanding of irregular transport coefficients in simple model systems. We use certain forms of the Green–Kubo formula as starting points for expansions of the diffusion coefficient in terms of correlated random walks. In section 2 we exemplify this approach for the piecewise linear map on the line studied in [3–5]. In section 3 we apply a suitably adapted version of it to diffusion in the periodic Lorentz gas. In both cases our approximations converge quickly to the precise diffusion coefficient as obtained from other numerical methods. We argue that for both models this approximation scheme provides a physical explanation for the irregular structure of these diffusion coefficients in terms of dynamical correlations, or memory effects. In section 4 we summarize our results and relate them to previous work on irregular and fractal transport coefficients.

2. Deterministic diffusion in one-dimensional maps on the line

Probably the simplest models exhibiting deterministic diffusion are one-dimensional maps defined by the equation of motion

$$x_{n+1} = M_a(x_n) \tag{1}$$

where $a \in \mathbb{R}$ is a control parameter and x_n is the position of a point particle at discrete time n. $M_a(x)$ is continued periodically beyond the interval $[0, 1)$ onto the real line by a lift of degree 1, $M_a(x+1) = M_a(x) + 1$. We assume that $M_a(x)$ is anti-symmetric with respect to $x = 0$, $M_a(x) = -M_a(-x)$. Let

$$m_a(x) := M_a(x) \mod 1 \tag{2}$$

be the reduced map related to $M_a(x)$. This map governs the dynamics on the unit interval according to $x_n = m_a^n(x)$. Let $\rho_n(x)$ be the probability density on the unit interval of an ensemble of moving particles starting at initial conditions $x \equiv x_0$. This density evolves according to the Frobenius–Perron continuity equation

$$\rho_{n+1}(x) = \int_0^1 \mathrm{d}y\, \rho_n(y)\delta(x - m_a(y)). \tag{3}$$

Here we are interested in the deterministic diffusion coefficient defined by the Einstein formula

$$D(a) = \lim_{n\to\infty} \left\langle (x_n - x_0)^2 \right\rangle \Big/ (2n) \tag{4}$$

with x_n governed by $M_a(x)$, where the brackets denote an average over the initial values x_0 with respect to the invariant probability density on the unit interval, $\langle \cdots \rangle := \int_0^1 \mathrm{d}x\, \rho^*(x) \cdots$. Equation (4) can be transformed onto the Green–Kubo formula for maps [1, 4, 14, 15],

$$D_n(a) = \sum_{k=0}^{n} c_k \langle j(x_0)\, j(x_k) \rangle \tag{5}$$

with $D(a) \equiv \lim_{n\to\infty} D_n(a)$ and

$$c_k = \begin{cases} \frac{1}{2} & k = 0 \\ 1 & k \geqslant 1. \end{cases} \tag{6}$$

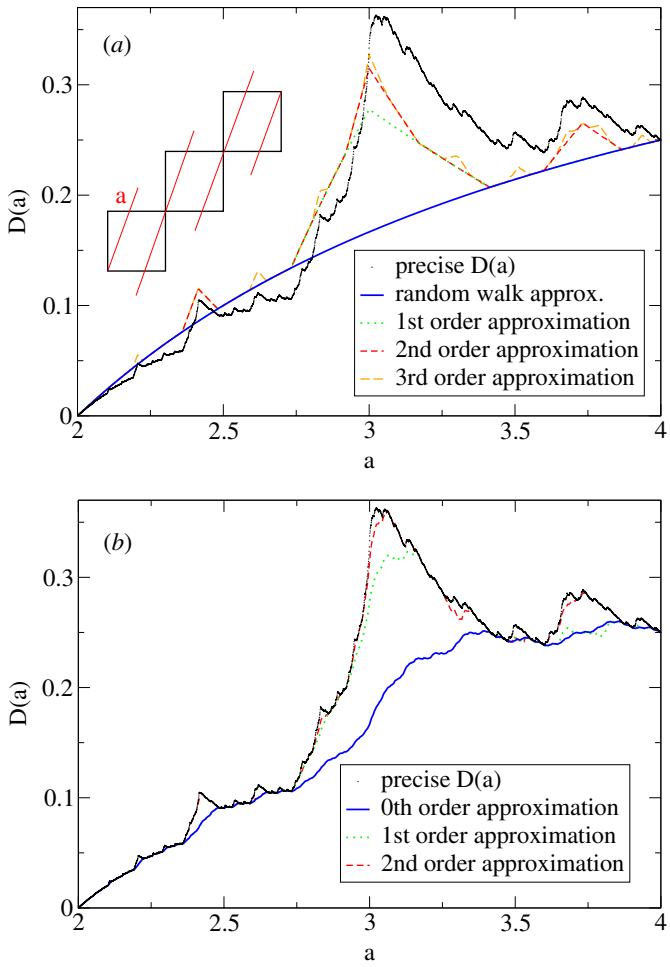

Figure 1. Diffusion coefficient $D(a)$ for the one-dimensional map shown in the upper left part of (a), where a is the slope of the map. The dots are obtained from the method of [3–5], the different lines correspond to different levels of approximations based on the Green–Kubo formula equation (5). In (a) the approximations were computed from equation (11) assuming a constant invariant density, and in (b) they are from equation (12) which includes the exact invariant density. Any error bars are smaller than visible. All quantities here and in the following figures are without units.

The jump velocity

$$j(x_n) := [x_{n+1}] - [x_n] \tag{7}$$

$[x]$ being the largest integer less than x, takes only integer values and denotes how many unit intervals a particle has traversed after one iteration starting at x_n. The map we study as an example is defined by

$$M_a(x) = \begin{cases} ax & 0 < x \leqslant \frac{1}{2} \\ ax + 1 - a & \frac{1}{2} < x \leqslant 1 \end{cases} \tag{8}$$

where the uniform slope $a > 2$ serves as a control parameter. The value for $M_a(0)$ follows from $M_a(1)$ by translational invariance. The Lyapunov exponent of this map is given by $\lambda(a) = \ln a$ implying that the dynamics is chaotic. A sketch of this map is shown in figure 1(a).

Figure 1 furthermore depicts the parameter-dependent diffusion coefficient of this map in the regime of $2 \leqslant a \leqslant 4$ as calculated in [3–5] by means of a numerical implementation of analytical methods. In these references numerical evidence that the irregularities on a fine scale are reminiscent of an underlying fractal structure was provided.

To analyse this fractal diffusion coefficient, equation (5) forms a suitable starting point because it distinguishes between two crucial contributions of the dynamics to the diffusion process, which are (1) the motion of the particle on the unit interval x_n mod 1 generating the invariant density $\rho_a^*(x)$, and (2) the integer jumps from one unit interval to another as related to $j(x_n)$. In fact, in [4, 11] it was shown that both parts are independent sources of fractality for the diffusion coefficient. However, in these references equation (5) was only discussed in the limit of infinite time. In this paper we suggest looking at the contributions of the single terms in this expansion, and analyse how the Green–Kubo formula approaches the exact diffusion coefficient step by step. We do this by systematically building up the hierarchies of approximate diffusion coefficients. These approximations should be defined such that the different dynamical contributions to the diffusion process are properly filtered out. Another issue is how to evaluate the single terms of the Green–Kubo expansion on an analytical basis. In this section we show how to do this for the one-dimensional model introduced above, in the next section we apply the same idea to billiards such as the periodic Lorentz gas.

We start by looking at the first term in equation (5). For $a < 4$ the absolute value of the jump velocity $j(x_n)$ is either 0 or 1. Assuming that $\rho_a^*(x) \simeq 1$ for $a \to 2$ and cutting off all higher order terms in equation (5), the first term leads to the well-known *random walk approximation* of the diffusion coefficient [4, 14, 16–18]

$$D_0(a) = \frac{1}{2}\int_0^1 \mathrm{d}x\; j^2(x) \tag{9}$$

which in case of map (8) reads

$$D_0(a) = (a-2)/(2a). \tag{10}$$

This solution is asymptotically correct in the limit of $a \to 2$. More generally speaking, the reduction of the Green–Kubo formula to the first term only is an exact solution for arbitrary parameter values only if all higher order contributions from the velocity autocorrelation function $C(n) := \langle j(x_0)\, j(x_n)\rangle$ are strictly zero. This is only true for systems of Bernoulli type [14]. Conversely, the series expansion in the form of equation (5) systematically gives access to higher order corrections by including higher order correlations, or memory effects. This leads us to the definition of two hierarchies of correlated random walk diffusion coefficients:

(1) Again, we make the approximation that $\rho_a^*(x) \simeq 1$. We then define

$$D_n^1(a) := \sum_{k=0}^{n} c_k \int_0^1 \mathrm{d}x\; j(x)\, j(x_k) \qquad n > 0 \tag{11}$$

with $D_0^1(a) \equiv D_0(a)$ given by equation (9). Obviously, this series cannot converge to the exact $D(a)$.

(2) By using the exact invariant density in the averages of equation (5) we define

$$D_n^\rho(a) := \sum_{k=0}^{n} c_k \int_0^1 \mathrm{d}x\; \rho_a^*(x)\, j(x)\, j(x_k) \qquad n > 0 \tag{12}$$

here with $D_0^\rho(a) = \frac{1}{2}\int_0^1 \mathrm{d}x\; \rho_a^*(x)\, j^2(x)$, which of course must converge exactly. The approximations $D_n^1(a)$ and $D_n^\rho(a)$ may be understood as time-dependent diffusion

coefficients according to the Green–Kubo formula (5). According to their definitions, $D_n^1(a)$ enables us to look at the contributions coming from $j(x_n)$ only, whereas $D_n^\rho(a)$ assesses the importance of contributions resulting from $\rho_a^*(x)$. The rates of convergence of both approximations give an estimate of how important higher order correlations are in the different parameter regions of the diffusion coefficient $D(a)$.

Similar to equation (10), equation (11) can easily be calculated analytically to first order reading

$$D_1^1(a) = \begin{cases} (a-2)/(2a) & 2 < a \leqslant 1+\sqrt{3} \quad \text{and} \quad 2+\sqrt{2} < a \leqslant 4 \\ 3/2 - 3/a - 2/a^2 & 1+\sqrt{3} < a \leqslant 3 \\ -1/2 + 3/a - 2/a^2 & 3 < a \leqslant 2+\sqrt{2}. \end{cases} \tag{13}$$

Further corrections up to order $n = 3$ were obtained from computer simulations, that is, an ensemble of point particles was iterated numerically according to equation (1). All results are contained in figure 1 showing that this hierarchy of correlated random walks generates a self-affine structure which resembles, to some extent, one of the well-known Koch curves. Figure 1(a) illustrates that this structure forms an important ingredient of the exact diffusion coefficient $D(a)$ thus explaining basic features of its fractality. Indeed, a suitable generalization of this approach in the limit of time to infinity leads to the formulation of $D(a)$ in terms of fractal generalized Takagi functions [4, 11].

Figure 1(b) depicts the results for the series of $D_n^\rho(a)$ up to order $n = 2$ as obtained from computer simulations. This figure illustrates that there exists a second source for an irregular structure related to the integration over the invariant density, as was explained above. In the Green–Kubo formula (5) both contributions are intimately coupled with each other via the integration over phase space.

We now perform a more detailed analysis to reveal the precise origin of the hierarchy of peaks in figure 1. For this purpose we redefine equation (11) as

$$D_n^1(a) = \int_0^1 \mathrm{d}x\; j(x) J_n(x) - \frac{1}{2}\int_0^1 \mathrm{d}x\; j^2(x) \qquad n > 0 \tag{14}$$

where we have introduced the *jump velocity function*

$$J_n(x) := \sum_{k=0}^{n} j(x_k) \tag{15}$$

again with $x \equiv x_0$. From equation (7) it follows that $J_n(x) = [x_{n+1}]$, that is, this function gives the integer value of the displacement of a particle starting at some initial position x. In figure 2 we depict some representative results for $J_1(x)$ under variation of the control parameter a. Because of the symmetry of the map we restrict our considerations to $0 < x < 0.5$. Equation (14) tells us that the product of this function with $j(x)$ determines the diffusion coefficient $D(a)$. The shaded bar in figure 2 marks the subinterval in which $j(x) = 1$, whereas $j(x) = 0$ otherwise, thus an integration over $J_1(x)$ on this subinterval yields the respective part of the diffusion coefficient. One can now relate the four diagrams (a) to (d) in figure 2 to the functional form of $D_1^1(a)$ in figure 1(a), thus understanding where the large peak in $D_1^1(a)$ for $2.732 < a < 3.414$ comes from: for $a < 2.732$, $J_1(x)$ does not change its structure and the interval where particles escape to other unit intervals increases monotonically, therefore $D(a)$ increases smoothly. However, starting from $a = 2.732$ particles can jump for the first time to next nearest neighbours within two time steps, as is visible in $J_1(x)$ taking values of 2 for x close to 0.5. Consequently, the slope of $D(a)$ increases drastically leading to the first large peak around $a = 3$. Precisely at $a = 3$, backscattering sets in meaning

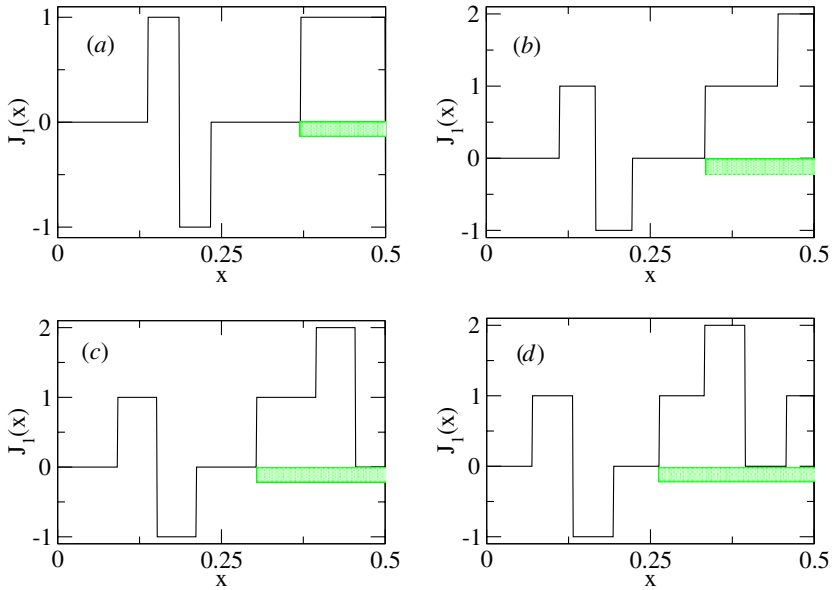

Figure 2. Jump velocity function $J_1(x)$ as defined by equation (15) which gives the integer value of the displacement of a particle starting at some initial position x. Shown are results for different values of the slope a: (a) $a = 2.7$, (b) $a = 3.0$, (c) $a = 3.3$, (d) $a = 3.8$. The shaded bar marks the subinterval where the jump velocity $j(x_n)$ defined in equation (7) is equal to one.

that particles starting around $x = 0.5$ jump back to the original unit interval within two time steps, as is reminiscent in $J_1(x)$ in the form of the region $J_1(x) = 0$ for x close to 0.5. This leads to the negative slope in $D(a)$ above $a = 3$. Finally, particles starting around $x = 0.5$ jump to the nearest neighbour unit intervals by staying there during the second time step instead of jumping back. This yields again a monotonically increasing $D(a)$ for $a > 3.414$. Any higher order peak for $D_n^1(a), n > 1$, follows from analogous arguments. Thus, the source of this type of fractality in the diffusion coefficient is clearly identified in terms of the topological instability of the function $J_1(x)$ under variation of the control parameter a. Indeed, this argument not only quantifies two previous heuristic interpretations of the structure of $D(a)$ as outlined in [3–5], it also explains why, on a very fine scale, there are still deviations between these results and the precise location of the extrema in $D(a)$, cf the 'overhang' at $a = 3$ as an example. The obvious reason is that contributions from the invariant density slightly modifying this structure are not taken into account.

Looking at the quantities $J_n(x)$ furthermore helps us to learn about the rates of convergence of the approximations $D_n^1(a)$ to $D(a)$ at fixed values of a, as is illustrated in figures 3(a)–(d). Here we have numerically calculated $J_n(x)$ at $a = 3.8$ for $n = 0, 1, 2, 3$. Again, the shaded bar indicates the region where $j(x) = 1$ enabling $J_n(x)$ to contribute to the value of the diffusion coefficient according to equation (14). In fact, $J_n(x)$ may also be interpreted as the *scattering function* of an ensemble of particles starting from the unit interval, since it sensitively measures the final position to which a particle moves within n time steps under variation of its initial position x. One can clearly see that, with larger n, $J_n(x)$ develops more and more discontinuities eventually leading to a highly singular and irregular function of x. Integration over further and further refinements of $J_n(x)$ determines the convergence of the series of $D_n^1(a)$ to a fixed value $D_\infty^1(a)$, cf figure 1(a). To obtain quantitative

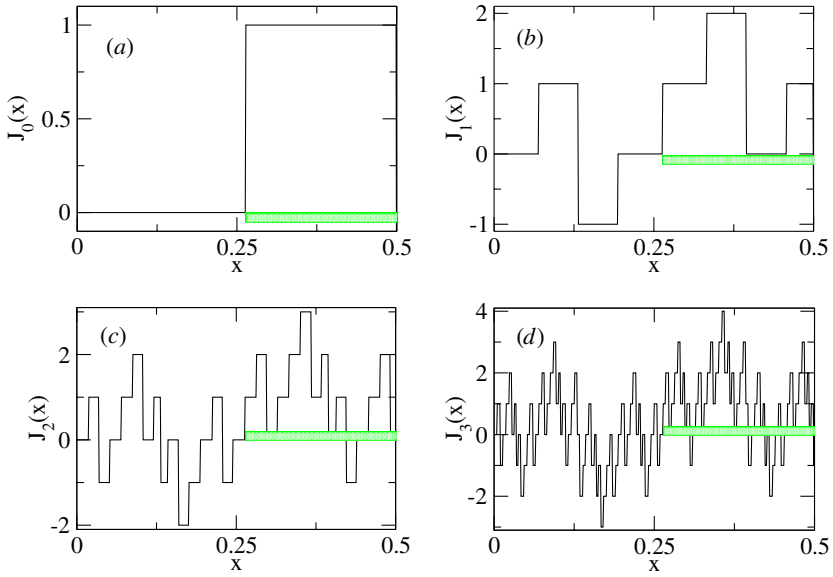

Figure 3. Jump velocity function $J_n(x)$ as defined by equation (15) at the fixed parameter value $a = 3.8$ for different numbers of time steps (*a*) $n = 0$, (*b*) $n = 1$, (*c*) $n = 2$, (*d*) $n = 3$. Again, the shaded bar marks the subinterval where the jump velocity $j(x_n)$ defined in equation (7) is equal to 1.

values for the associated rates of convergence with respect to parameter variation is an open question.

We remark that a suitable integration over the functions $J_n(x)$ leads to the definition of fractal so-called generalized Takagi functions, which can be calculated in terms of de Rham-type functional recursion relations [4, 11]. In a way, the integration over jump velocity functions such as the one shown in figure 3(*d*) is similar to the integration over Cantor set structures leading to Devil's staircase-type functions [19]. Our results presented so far thus bridge the gap between understanding the coarse functional behaviour of $D(a)$ on the basis of simple random walk approximations only, and analysing its full fractal structure in terms of Takagi-like fractal forms, in combination with an integration over a complicated non-uniform invariant density. We now show that essentially the same line of argument can be successfully applied to more physical dynamical systems such as particle billiards.

3. Deterministic diffusion in billiards

The class of two-dimensional billiards we want to discuss here is described as follows: a point particle undergoes elastic collisions with obstacles of the same size and shape whose centres are fixed on a triangular lattice. There is no external field, thus the equations of motion are defined by the Hamiltonian $H = mv^2/2$ supplemented by geometric boundary conditions as induced by the scatterers. A standard example is the periodic Lorentz gas for which the scatterers consist of hard disks of radius R, see figure 4 [1, 2]. In the following we choose $m = 1$, $v = 1$, $R = 1$, and as a control parameter we introduce the smallest inter-disk distance w such that the lattice spacing of the disks is $2 + w$. w is related to the number density n of the disks by $n(w) = 2/[\sqrt{3}(2 + w)^2]$. At close packing $w = 0$ the moving particle is trapped in a single triangular region formed between three disks, see figure 4, part (1).

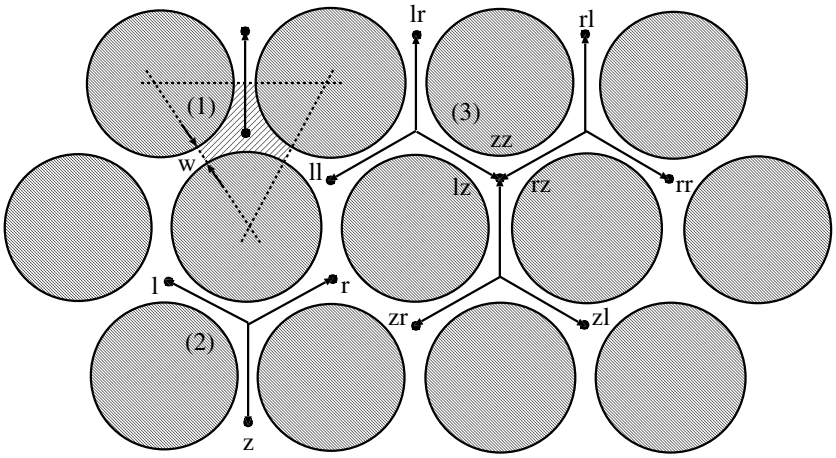

Figure 4. Geometry of the periodic Lorentz gas with the gap size w as control parameter. The hatched area related to (1) marks a so-called trapping region, the arrow gives the lattice vector connecting the centre of this trap to the next one above. In (2) three lattice vectors are introduced and labelled with the symbols l, r, z. They indicate the positions where particles move along the hexagonal lattice of Wigner–Seitz cells, starting from the trap z, within two time steps of length τ. (3) depicts the situation after three time steps τ with different lattice vectors associated with symbol sequences of length 2.

For $0 < w < w_\infty = 4/\sqrt{3} - 2 = 0.3094$, the particle can move across the entire lattice, but it cannot move collision-free for an infinite time. For $w > w_\infty$ the particle can move ballistic-like in the form of arbitrarily far jumps between two collisions.

The diffusion coefficient for this particle billiard can be defined by the two-dimensional equivalent of the Einstein formula (4) reading

$$D(w) = \lim_{t\to\infty} \langle (\boldsymbol{x}(t) - \boldsymbol{x}(0))^2 \rangle / (4t) \tag{16}$$

where, again, the average is taken over the equilibrium distribution of particles with position coordinates $\boldsymbol{x}(t)$. It can be proved that in the regime of $0 < w < w_\infty$ the parameter-dependent diffusion coefficient $D(w)$ exists [20]. The full parameter-dependence of this function was discussed particularly in [9] showing that, on a fine scale, $D(w)$ is an irregular function of the parameter w similar to the diffusion coefficient of the one-dimensional map $D(a)$ as discussed above. Whether $D(w)$ is indeed fractal, or maybe C^1 but not C^2 in contrast to the one-dimensional map discussed above, is currently an open question. The main issue we want to focus on in this section is quantitative approximations for the full parameter dependence of $D(w)$, and to check for the importance of memory effects. A first simple analytical approximation for the diffusion coefficient was derived by Machta and Zwanzig in [21]. This solution was based on the assumption that diffusion can be treated as a Markovian hopping process between the triangular trapping regions indicated in figure 4. For random walks on two-dimensional isotropic lattices the diffusion coefficient then reads $D = \ell^2/(4\tau)$, where $\ell = (2 + w)/\sqrt{3}$ is the smallest distance between two centres of the traps, and τ^{-1} is the average rate at which a particle leaves a trap. This rate can be calculated by the fraction of phase space volume available for leaving the trap divided by the total phase space volume of the trap thus leading to the Machta–Zwanzig random walk approximation of the diffusion coefficient

$$D_{\mathrm{MZ}}(w) = \frac{w(2+w)^2}{\pi[\sqrt{3}(2+w)^2 - 2\pi]}. \tag{17}$$

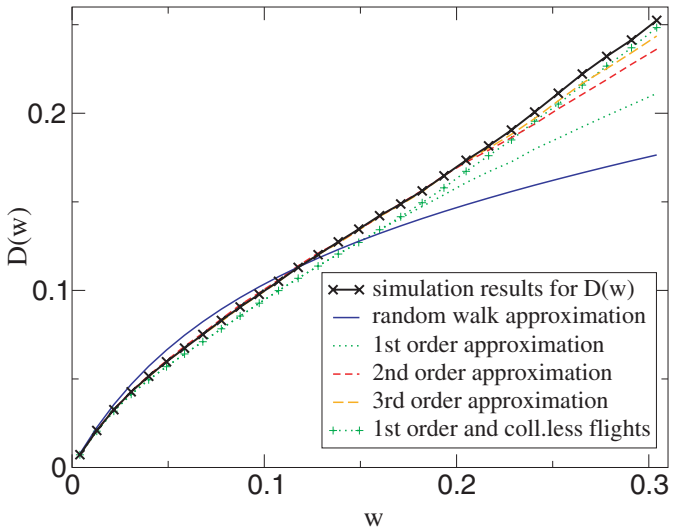

Figure 5. Diffusion coefficient $D(w)$ for the periodic Lorentz gas as a function of the gap size w as a control parameter. The computer simulation results for $D(w)$ are from [8], error bars are much smaller than the size of the symbols. The other lines correspond to different levels of approximation (19), the last approximation (again with symbols) is from equation (23).

Indeed, this approximation is precisely the billiard analogue to the one-dimensional random walk diffusion coefficient for maps (9), (10). Similarly, this approximation is asymptotically exact only for $w \to 0$, as is shown in comparison to computer simulation results in figure 5 [9, 21].

In [9], equation (17) was systematically improved by including higher order correlations. Two basic approaches were presented both starting from the idea of Machta and Zwanzig of looking at diffusion in the Lorentz gas as a hopping process on a hexagonal lattice of 'traps' with frequency τ^{-1}. This picture was quantified by introducing a simple symbolic dynamics for a particle moving from trap to trap as indicated in figure 4. Let us follow a long trajectory of a particle starting with velocity $\boldsymbol{v}$ parallel to the y-axis, cf (1) in figure 4. For each visited trap we label the entrance through which the particle entered with z, the exit to the left of this entrance with l, and the one to the right with r, see (2) in figure 4. Thus, a trajectory in the Lorentz gas is mapped onto words composed of the alphabet $\{z, l, r\}$. One can now associate transition probabilities with these symbol sequences reading, for a time interval of 2τ, $p(z)$, $p(l)$, $p(r)$. $p(z)$ corresponds to the probability of backscattering, whereas $p(l) = p(r) = (1 - p(z))/2$ indicates forward scattering. For a time interval of 3τ, we have nine symbol sequences each consisting of two symbols leading to the probabilities $p(zz)$, $p(zl)$, $p(zr)$, $p(lz)$, $p(ll)$, $p(lr)$, $p(rz)$, $p(rl)$, $p(rr)$. Besides this hierarchy of conditional probabilities defined on a symbolic dynamics there is a different type of probability that a particle leaving a trap jumps without any collision directly to the next nearest neighbour trap. As was shown in [9], equation (17) can be corrected by analytically including all these probabilities. Alternatively, lattice gas computer simulations were performed by using the probabilities as associated with the symbol sequences. The heuristic corrections of equation (17) led to a satisfactory explanation of the overall behaviour of $D(w)$ on a coarse scale, however, the convergence was not exact. The lattice gas simulations, on the other

hand, were converging exactly, however, here a proper analytical expression for the diffusion coefficient approximations in terms of the associated probabilities was not available.

In analogy with the procedure as outlined for the one-dimensional map, that is, starting from a suitable Green–Kubo formula, we will now define a third approximation scheme that we expect to be generally applicable to diffusion in particle billiards. Compared to the two existing approaches mentioned above the advantage of the new method is two-fold, namely (1) that by using the set of symbolic probabilities the respective Green–Kubo formula can be evaluated according to an analytical scheme, and (2) that the resulting approximations converge exactly to the computer simulation results.

In the appendix we prove that, starting from the Einstein formula (16), quite in analogy with the one-dimensional case a Green–Kubo formula can be derived that is defined for an ensemble of particles moving on the hexagonal lattice of traps depicted in figure 4. The result reads

$$D(w) = \frac{1}{2\tau}\sum_{k=0}^{\infty} c_k \langle \boldsymbol{j}(\boldsymbol{x}_0)\cdot\boldsymbol{j}(\boldsymbol{x}_k)\rangle \tag{18}$$

again with c_k as defined in equation (6). Here $\boldsymbol{j}(\boldsymbol{x}_k)$ defines jumps at the kth time step in terms of the lattice vectors $\boldsymbol{\ell}_{\alpha\beta\gamma\ldots}$ associated with the respective symbol sequence of the full trajectory on the hexagonal lattice, cf figure 4. Let us start with $\boldsymbol{j}(\boldsymbol{x}_0) = \boldsymbol{\ell}/\tau$, $\boldsymbol{\ell} := (0, \ell)^*$. The next jumps are then defined by $\boldsymbol{j}(\boldsymbol{x}_1) = \boldsymbol{\ell}_\alpha/\tau$, $\alpha \in \{l, r, z\}$, and so on. The averages indicated in equation (18) by the brackets are calculated by weighting the respective scalar products of lattice vectors with the corresponding conditional probabilities $p(\alpha\beta\gamma\cdots)$. Note that equation (18) is the honeycomb lattice analogue to the Green–Kubo formula derived by Gaspard for the Poincaré–Birkhoff map of the periodic Lorentz gas [2, 22]. The Poincaré–Birkhoff version is very efficient for numerical computations; however, according to its construction it fails to reproduce the Machta–Zwanzig approximation (17). Consequently, it does not appear to be very suitable for diffusion coefficient approximations of low order. More details will be discussed elsewhere [23]. We remark that, in terms of using a symbolic dynamics, there is also some link between equation (18) and respective diffusion coefficient formulae obtained from periodic orbit theory [24, 25].

We now demonstrate how equation (18) can be used for systematic improvements of the diffusion coefficient on the lattice of traps by including dynamical correlations: as in the case of one-dimensional maps we start by looking at the first term in equation (18) and cut off all higher order contributions. Obviously, the first term is again the random walk expression for the diffusion coefficient on the hexagonal lattice of traps that, by including the respective solution for the jump frequency τ^{-1}, boils down to equation (17). For calculating higher order corrections we now define the hierarchy of approximations

$$D_n(w) = \frac{l^2}{4\tau} + \frac{1}{2\tau}\sum_{\alpha\beta\gamma\ldots} p(\alpha\beta\gamma\cdots)\boldsymbol{\ell}\cdot\boldsymbol{\ell}(\alpha\beta\gamma\cdots) \qquad n > 0 \tag{19}$$

with $D_0(w)$ given by equation (17). To our knowledge there is no method yet available to analytically calculate the conditional probabilities $p(\alpha\beta\gamma\cdots)$. Our following evaluations are therefore based on the data presented in [9] as obtained from computer simulations. In terms of the formal probabilities it is now easy to calculate the solution for the first order approximation at time step 2τ as

$$D_1(w) = D_0(w) + D_0(w)(1 - 3p(z)). \tag{20}$$

For a comparison of this formula with the simulation data $D(w)$, see figure 5. We remark that the corresponding solution in [9] as obtained from a heuristical correction of equation (17)

reads $D_{1,\mathrm{MZ}}(w) = D_0(w)3(1 - p(z))/2$. Indeed, one can show that the new formula (20) is closer to $D(w)$ for large w, whereas for small w the previous approximation is somewhat better. It is straightforward to calculate the two approximations of next higher order as

$$D_2(w) = D_1(w) + D_0(w)\,(2p(zz) + 4p(lr) - 2p(ll) - 4p(lz)) \tag{21}$$

and as

$$\begin{aligned} D_3(w) = D_2(w) + D_0(w)[&p(llr) + p(llz) + p(lrl) + p(lrr) + p(lzl) + p(lzz) + p(rll) \\ &+ p(rlr) + p(rrl) + p(rrz) + p(rzr) + p(rzz) + p(zll) + p(zlz) + p(zrr) \\ &+ p(zrz) + p(zzl) + p(zzr) - 2(p(lll) + p(lrz) + p(lzr) + p(rlz) + p(rrr) \\ &+ p(rzl) + p(zlr) + p(zrl) + p(zzz))]. \end{aligned} \tag{22}$$

All results are shown in figure 5 demonstrating that the series of approximations defined by equation (19) converges quickly and everywhere to the simulation results. Our new scheme thus eliminates the deficiency of the semi-analytical approximation proposed in [9] that was based on heuristically correcting the Machta–Zwanzig approximation (17). By comparing this new scheme with the lattice gas simulations of the same reference, on the other hand, it turns out that the rate of convergence of the lattice gas approach is still a bit better. In any case, all these three methods unambiguously demonstrate that for achieving a complete understanding of the density-dependent diffusion coefficient in the periodic Lorentz gas it is unavoidable to take higher order correlations, or the impact of memory effects, properly into account.

We finally remark that a very good low-order approximation for the diffusion coefficient can already be obtained by combining equation (20) with the probability of collisionless flights $p_{\mathrm{cf}}(w)$ mentioned above, that is, by taking into account the possibility of next nearest neighbour jumps. The correction of $D_0(w)$ as given by equation (17) according to collisionless flights only was already calculated in [9] and reads $D_{0,\mathrm{cf}}(w) = D_0(w)(1 + 2p_{\mathrm{cf}}(w))$. Adding now the second term of equation (20) to this expression by just following the Green–Kubo scheme yields

$$D_{1,\mathrm{cf}}(w) = D_0(w)(2 + 2p_{\mathrm{cf}}(w) - 3p(z)). \tag{23}$$

This solution is also depicted in figure 5 and shows that this approximation indeed significantly improves equation (20) for large w yielding a function that is qualitatively and quantitatively very close to $D(w)$. We know of no better approximation for $D(w)$ based on information such as $p(z)$ and $p_{\mathrm{cf}}(w)$ only. The successful application of equation (23) suggests that collisionless flights form an important mechanism to understand the full diffusive dynamics of this billiard. However, somewhat surprisingly they are not explicitly contained neither in the Green–Kubo expansion (19) nor in the lattice gas simulations of [9]. In both cases exact convergence is achieved by following the hierarchy of symbol sequence probabilities only in which collisionless flights are not apparent.

4. Summary and conclusions

In this paper we suggested a general scheme of how to understand the structure of parameter-dependent deterministic diffusion coefficients in simple model systems. The important point was to find suitable Green–Kubo formulae to start with. We used the fact that the class of models we studied here was defined on periodic lattices, and respectively we discretized the dynamics of the moving particles according to these lattices. As two different examples we analysed a simple one-dimensional map on the line as well as the periodic Lorentz gas. In both cases we recovered the respective well-known random walk formulae for the diffusion

coefficient as zero-order approximations in our Green–Kubo approach. We then calculated higher order terms according to Green–Kubo thus systematically including higher order correlations. As much as possible this analysis was performed analytically, alternatively in combination with data obtained from computer simulations. Our results provided clear evidence that a proper understanding of the parameter-dependent diffusion coefficients in both models can only be achieved by taking strong memory effects into account. In this respect our research appears to be somewhat related to the findings of long-time tails in the velocity autocorrelation function of simple model systems such as Lorentz gases, and to the existence of non-analyticities in the density expansion of transport coefficients, which are both consequences of strong correlations in the dynamics of the moving particles; see [26] for a nice review from the side of kinetic theory and [2, 9] for a possible connection to the specific questions discussed here. In the case of the one-dimensional map our approach enables a detailed understanding of the dynamical mechanism generating the most pronounced irregularities in the fractal diffusion coefficient. In the case of the periodic Lorentz gas this scheme straightforwardly generalizes the Machta–Zwanzig random walk formula in terms of systematic higher order approximations that converge exactly to the simulation results. We may emphasize again at this point that, although the diffusion coefficient for the periodic Lorentz gas as presented in figure 5 appears to be rather smooth, magnifications of this curve unambiguously reveal the existence of irregularities on fine scales [9].

For one-dimensional maps the infinite time limit of this approach, though not the intermediate level as quantitatively discussed here, was already worked out in [4, 11] leading to the definition of the diffusion coefficient in terms of fractal so-called generalized Takagi functions. For the periodic Lorentz gas an analogous generalization would be desirable as well. We furthermore remark that the approximation scheme as presented in this paper was already successfully applied (1) to the one-dimensional climbing sine map, where there is a complicated transition scenario between normal and anomalous diffusion [27], and (2) to the so-called flower shape billiard, where the hard discs of the Lorentz gas are replaced by obstacles of flower shape [28]. In both cases the resulting parameter-dependent diffusion coefficients, as far as they exist, are much more complicated functions than in the corresponding models discussed above, yet our scheme yields systematic explanations of the structure of these functions in terms of strong dynamical correlations. We thus expect that using Green–Kubo formulae this way provides a general access road to understanding deterministic diffusion in low-dimensional periodic arrays of scatterers, possibly also in view of experimental results on systems such as antidot lattices, ratchets and Josephson junctions.

Acknowledgments

We thank T Harayama for interesting discussions, L Matyas for a careful reading of the manuscript, and Chr Dellago for originally having generated the dataset that was used for the Lorentz gas.

Appendix A. Green–Kubo formula on the hexagonal lattice

In this appendix we derive equation (18) that yields the diffusion coefficient $D(w)$ for the periodic Lorentz gas via a generalization of the Machta–Zwanzig picture. That is, we look at diffusion as a higher order Markov process on a hexagonal lattice of traps with lattice spacing ℓ where particles hop with frequency τ^{-1} from trap to trap, cf figure 4. The time t is suitably rewritten in terms of the escape time $\tau = (\pi/6w)(\sqrt{3}/2(2+w)^2 - \pi)$ [21] as $t = n\tau, n \in N$.

Let $\boldsymbol{x}_n$ be the position of the moving particle at time step n. We then write $\boldsymbol{x}_n \equiv \boldsymbol{X}_n + \tilde{\boldsymbol{x}}_n$, where $\boldsymbol{X}_n$ denotes the position of the trap on the hexagonal lattice in which the particle is situated at time step n. This vector can be expressed by a suitable combination of lattice vectors. For example, one may choose a sum of $\boldsymbol{\ell}_{\alpha\beta\gamma\ldots}$ as introduced in section 3, see figure 4; a more precise definition is not necessary here. Correspondingly, $\tilde{\boldsymbol{x}}_n$ is the distance from the nearest trap centre to the actual position of the particle in the Wigner–Seitz cell.

The Einstein formula (16) then reads

$$D(w) = \lim_{n\to\infty} \left\langle (\boldsymbol{X}_n + \boldsymbol{\Delta}\tilde{\boldsymbol{x}}_n)^2 \right\rangle \Big/ (4n\tau) \tag{A1}$$

where $\boldsymbol{\Delta}\tilde{\boldsymbol{x}}_n := \tilde{\boldsymbol{x}}_n - \tilde{\boldsymbol{x}}_0$. Multiplying the nominator we get

$$\left\langle \boldsymbol{X}_n^2 + 2\boldsymbol{X}_n \cdot \boldsymbol{\Delta}\tilde{\boldsymbol{x}}_n + \boldsymbol{\Delta}\tilde{\boldsymbol{x}}_n^2 \right\rangle. \tag{A2}$$

According to its definition the last term is bounded, $\boldsymbol{\Delta}\tilde{\boldsymbol{x}}_n^2 < \text{const}$. To the second term we apply the Hölder inequality [29] yielding

$$|\langle \boldsymbol{X}_n \cdot \boldsymbol{\Delta}\tilde{\boldsymbol{x}}_n \rangle| \leqslant \sqrt{\langle |\boldsymbol{X}_n|^2 \rangle} \sqrt{\langle |\boldsymbol{\Delta}\tilde{\boldsymbol{x}}_n|^2 \rangle} < \text{const} \sqrt{\langle |\boldsymbol{X}_n|^2 \rangle}. \tag{A3}$$

Consequently, in the limit of infinite time only the first term in equation (A2) contributes to the positive diffusion coefficient $D(w)$ of equation (A1) leading to

$$D(w) = \lim_{n\to\infty} \left\langle \boldsymbol{X}_n^2 \right\rangle \Big/ (4n\tau). \tag{A4}$$

Starting from this Einstein formula on the hexagonal lattice it is now straightforward to derive equation (18). $\boldsymbol{X}_n^2 = X_n^2 + Y_n^2$ tells us that essentially there are two one-dimensional parts, thus we are back to the respective derivation of equation (5) in [1]. To make this precise, let us write

$$X_n = \sum_{k=0}^{n-1} j(x_k) \tag{A5}$$

which is in analogy with equation (15). However, here $j(x_k) := X_{k+1} - X_k$ is strictly speaking no jump *velocity*, since it only denotes the distance a particle jumps within a time interval τ, whereas $\tau = 1$ in equation (7). Multiplying out the nominator of equation (A4) in terms of equation (A5) leads to an equation for $D(w)$ in the form of velocity autocorrelation functions $C(k,l) := \langle j(x_k) \cdot j(x_l) \rangle = \int \mathrm{d}x\, \mathrm{d}y\, \rho^*(x,y) j(x_k) \cdot j(x_l)$, where $\rho^*(x,y)$ is the equilibrium density of the periodic Lorentz gas. Translational invariance implies $C(k,l) = C(0, l-k)$ which is easily shown by substitution combined with conservation of probability according to the Frobenius–Perron equation of the billiard. Summing up all contributions $C(0,k)$ obtained from the multiplication, doing the same for the component Y_n, and putting both results together yields equation (18).

References

[1] Dorfman J R 1999 *An Introduction to Chaos in Nonequilibrium Statistical Mechanics* (Cambridge: Cambridge University Press)

[2] Gaspard P 1998 *Chaos, Scattering, and Statistical Mechanics* (Cambridge: Cambridge University Press)

[3] Klages R and Dorfman J R 1995 *Phys. Rev. Lett.* **74** 387

[4] Klages R 1996 *Deterministic Diffusion in One-Dimensional Chaotic Dynamical Systems* (Berlin: Wissenschaft & Technik)

[5] Klages R and Dorfman J R 1999 *Phys. Rev.* E **59** 5361

[6] Dana I, Murray N and Percival I 1989 *Phys. Rev. Lett.* **65** 1693

[7] Rechester A and White R 1980 *Phys. Rev. Lett.* **44** 1586

[8] Leboeuf P 1998 *Physica* D **116** 2767

[9] Klages R and Dellago C 2000 *J. Stat. Phys.* **101** 145
[10] Harayama T and Gaspard P 2001 *Phys. Rev.* E **64** 036215
[11] Gaspard P and Klages R 1998 *Chaos* **8** 409
[12] Moran B and Hoover W 1987 *J. Stat. Phys.* **48** 709
[13] Weiss D *et al* 1991 *Phys. Rev. Lett.* **66** 2790
[14] Fujisaka H and Grossmann S 1982 *Z. Phys.* B **48** 261
[15] Gaspard P 1992 *J. Stat. Phys.* **68** 673
[16] Geisel T and Nierwetberg J 1982 *Phys. Rev. Lett.* **48** 7
[17] Schell M, Fraser S and Kapral R 1982 *Phys. Rev.* A **26** 504
[18] Klages R and Dorfman J R 1997 *Phys. Rev.* E **55** R1247
[19] Mandelbrot B 1982 *The Fractal Geometry of Nature* (San Francisco, CA: Freeman)
[20] Bunimovich L A and Sinai Y G 1980 *Commun. Math. Phys.* **78** 247
[21] Machta J and Zwanzig R 1983 *Phys. Rev. Lett.* **50** 1959
[22] Gaspard P 1996 *Phys. Rev.* E **53** 4379
[23] Harayama T unpublished
[24] Cvitanović P, Eckmann J-P and Gaspard P 1995 *Chaos Solitons Fractals* **6** 113
[25] Cvitanovic P, Gaspard P and Schreiber T 1992 *Chaos* **2** 85
[26] Dorfman J R and van Beijeren H 1977 *Statistical Mechanics* vol B ed B Berne (New York: Plenum) ch 3 pp 65–179
[27] Korabel N and Klages R unpublished
[28] Harayama T, Klages R and Gaspard P 2002 *E-print* nlin.CD/0204046
[29] Lasota A and Mackey M 1994 *Chaos, Fractals, and Noise. (Applied Mathematical Sciences vol 97)* 2nd edn (Berlin: Springer)